Seismic Waveform Tomography: crosshole results from the Nimr field in Oman

R. G. Pratt, Queen's University, Kingston, Ontario; R.E. Plessix, W.A. Mulder, Shell Int'l E & P, The Hague*

Summary

We describe the waveform tomographic inversion of seismic crosshole data from the Nimr field in Oman. Our initial ray-theoretical inversions of the traveltimes suggest a low level of P-wave anisotropy, as do our initial, long-wavelength waveform inversion results. Higher resolution, 2-D waveform inversions that include this low level of background anisotropy are successful in predicting the observed data, but the velocity models are smoother than expected. Surprisingly, similar waveform inversions that do not include any anisotropy are also successful in modelling the observed data. These latter inversions yield velocity models with far stronger velocity contrasts in the thin layers recovered during the 2-D inversions. We conclude that the anisotropy is primarily layer-induced, and that when an isotropic approach is used a long-wavelength anisotropy is "created" during the inversion.

Introduction

The geometry of the crosshole survey in the Nimr field is shown in Figure 1, together with the sonic logs and a representative shot gather (after Goudswaard et al, 1998). Our objective was to obtain models of the acoustic velocity field that would adequately explain the observed data, including the direct arrivals, diffractions, reflections, guided waves, etc. Our methodology utilizes a frequency-domain finite difference numerical solution of the acoustic wave equation (Pratt, 1990) to generate forward solutions for each trial velocity model. The velocity model is iteratively improved until a good match is obtained between synthetic and observed data, frequency by frequency (Song et al, 1995; Pratt, 1999).

Traveltime tomography

An initial model constructed using ray-theoretical traveltime methods for anisotropic media (Pratt and Chapman, 1992) provides an indication that a low level of P-wave anisotropy is affecting the arrival times (Figure 2). A layered velocity structure is obtained that corresponds closely to a smoothed version of the well logs, but in order to obtain this structure approximately 6-8% anisotropy was

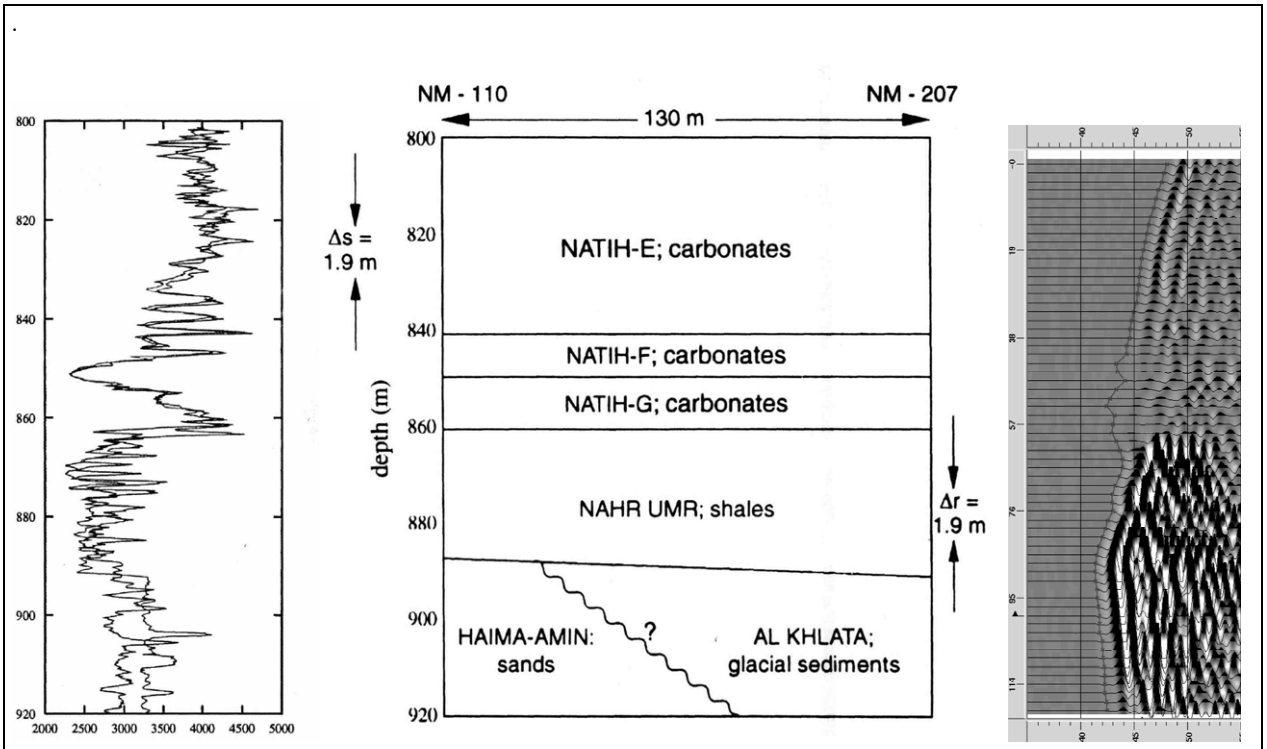

Figure 1: a) Sonic logs from source and receiver wells; the velocities are slightly lower in the Haima-Amin sands, b) survey geometry and stratigraphy, c) sample shot data (shot depth 897 m), with first arrival picks.

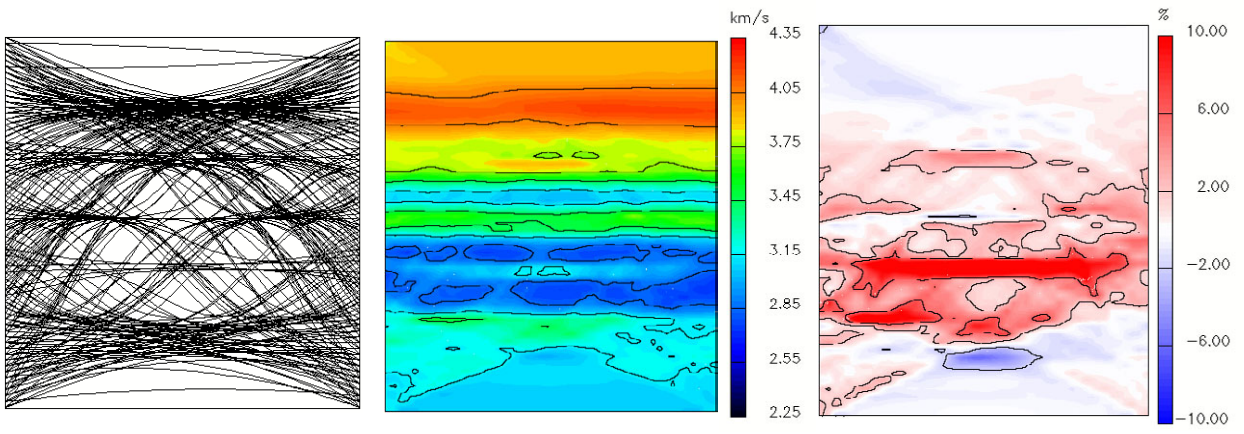

Figure 2 Anisotropic traveltime inversion result. a) ray paths traced in a model created by interpolation of smoothed sonic logs, b) velocity tomogram and c) anisotropy tomogram (an image of epsilon, the fractional difference between horizontal and vertical velocities).

required in some parts of the model. The final traveltime residuals for this model have an RMS level of 0.6 ms.

Waveform tomography

We begin our waveform inversion procedure using the traveltime results of Figure 2(b) as a starting model. Anisotropy can distort the velocity images in tomography and we therefore introduce a background level of anisotropy into the models. Because our forward model is acoustic, we simulate the anisotropy by using a geometrical "stretch" of the coordinates. Although we thus only simulate elliptic anisotropy, this is adequate at low levels of anisotropy. In any case this should be an improvement over isotropic inversions. We studied the objective function as the background level of anisotropy was varied: for these smooth initial models we observed a slight decrease in misfit at a background level of anisotropy of 10%, which seems to confirm the traveltime results.

Nevertheless, the anisotropy in our model is now homogeneous. In order to prevent artifacts related to the true spatial anisotropy distribution, the initial inversions were carried out using a one-dimensional (1-D) parameterization. The inversion is relaxed to two dimensions (2-D) only toward the end of the iteration schedule.

The waveform inversion procedure requires several processing decisions to be made:

1. We window the input data within a short time window beginning with the picked arrival times. The window width is initially very short (3 ms), to allow the model to initially fit the direct arrivals. Later the window width is expanded to 13 ms in order to fit the later reflections, diffractions and other scattered events.

2. We apply amplitude normalization within the data window to ensure that even weak picked arrivals are well represented within the input data. In the final stages of the inversion we change to true amplitude data.

3. We select a schedule of frequencies for inversion. In this case the data bandwidth is approximately 200 – 2000 Hz, and we selected the frequencies between these 200-1000 Hz with a 50 Hz discretization interval, starting with the lowest frequencies and finishing with the highest. This allows a full description of 1/50 Hz = 20 ms of the data in the time domain, up to 1000 Hz.

4. We choose a "reduced parameterization schedule" in which the number of grid points in the model at each iteration is specified. Our schedule begins with Nx=2, and Nz increases from 10 to 100. This allows the 1-D components of the model to be resolved before we attempt to solve for the 2-D variations. During the later stages the parameterization is gradually changed to become fully 2-D (with Nx=100 and Nz = 100).

5. We obtain an initial source wavelet directly from the data, by time shifting and stacking the direct arrivals. This wavelet is used until the very late stages of the inversion, when the source variation is included in the inversion parameters.

Our final, anisotropic model, obtained using frequencies from 200 – 1000 Hz, predicts many of the features of the observed data (Figure 3b vs Figure 3a). In particular the

direct arrivals are extremely well matched, although some of the later, guided arrivals are not as well predicted. The apparent resolution is consistent with the wavelength of the survey and the velocity variations are well matched with those of the original sonic log. A detailed comparison with the sonic logs (Figure 4, left) shows that some of the velocity variations for the receiver well (red) are not completely recovered. Indeed, these velocity results also differ from the previous results (Goudswaard et al., 1998; Plessix, 2000).

An alternative velocity model was obtained from the same data, with the same inversion strategy but using a completely isotropic model. This model appears to fit the data nearly as well (Figure 3c vs Figure 3a and 3b). In contrast to the anisotropic inversion, the velocity structure (Figure 5) recovered in this case exhibits much stronger and more detailed heterogeneity. We encounter slightly more difficulties in matching sonic velocities between depth 890 m and 920 m . A detailed examination of this shot gather (and others not shown here), indicates that the reflections and other scattered arrivals are somewhat stronger in the isotropic model than in the anisotropic model.

Conclusion

We conclude that the anisotropy observed on the traveltimes and on the initial waveform inversions can be modelled in two alternative fashions: we may either introduce a background level of anisotropy (and recover a smooth model), or we may constrain the model to be isotropic. In the latter case the inversion constructs a more heterogeneous velocity model in which the velocity variations are sufficient to create an effective anisotropy for the traveltimes, and for the direct arrival waveforms.

References

Goudsward, J.C.M., ten Kroode, A.P.E., Snieder, R.K. and Verdel, A.R., 1998, Detection of lateral velocity contrasts by crosswell traveltime tomography. Geophysics, **63**, 523-533.

Plessix, R.E., 2000, Automatic crosswell tomography: an application of the differential semblance optimization to two examples, Geophysical Prospecting, **48** (5), pp.937-951.

Pratt, R. G., 1990, Frequency domain elastic wave modeling by finite differences: A tool for cross-hole seismic imaging. Geophysics, **55**, 626-632.

Pratt, R.G. 1999, Seismic waveform inversion in the frequency domain, Part1: Theory and verification in a physical scale model. Geophysics, **64**, 888-901.

Pratt, R.G., and Chapman, C.H., 1992, Traveltime tomography in anisotropic media-II. Application: Geophysical Journal International, **109**, 20-37.

Song, Z.M,. Williamson, P.R. and Pratt, R.G., 1995, Frequency domain acoustic wave modelling and inversion of crosshole data II – Inversion method, synthetic experiments and real-data results: Geophysics, **60**, 796-809.

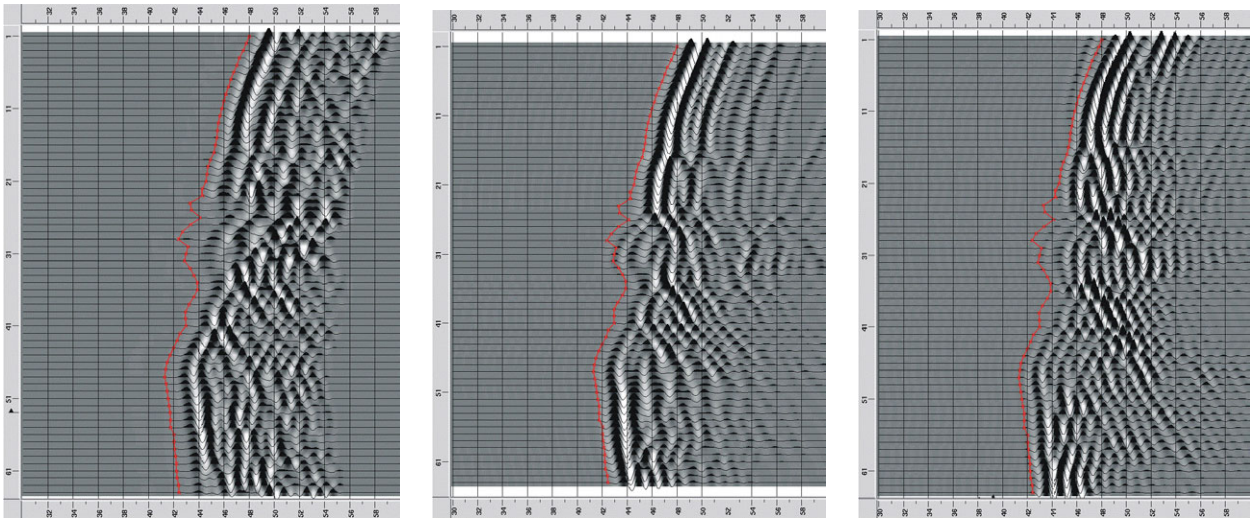

a) b) c)

Figure 3: a) Shot gather from field data b) synthetic shot gather (10% anisotropy) c) synthetic shot gather (isotropy). The traveltime picks (red) are consistent between Figures.

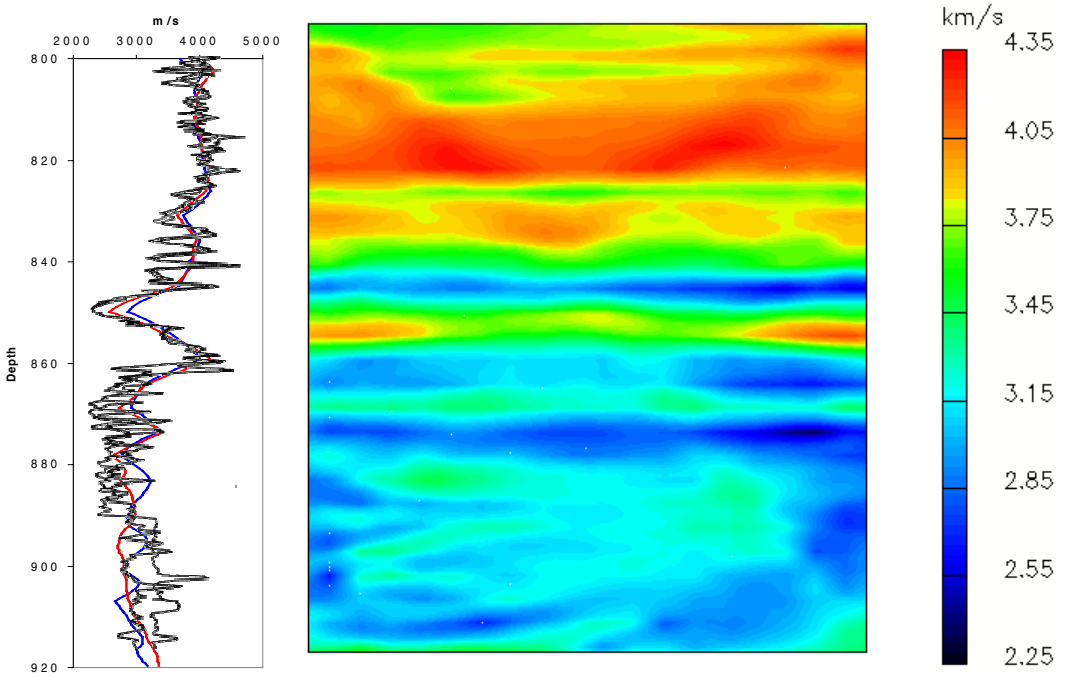

Figure 4: Final anisotropic (10%) waveform inversion result. The result at the well locations (red = receiver well) is shown on the left together with the original sonic velocities (black).

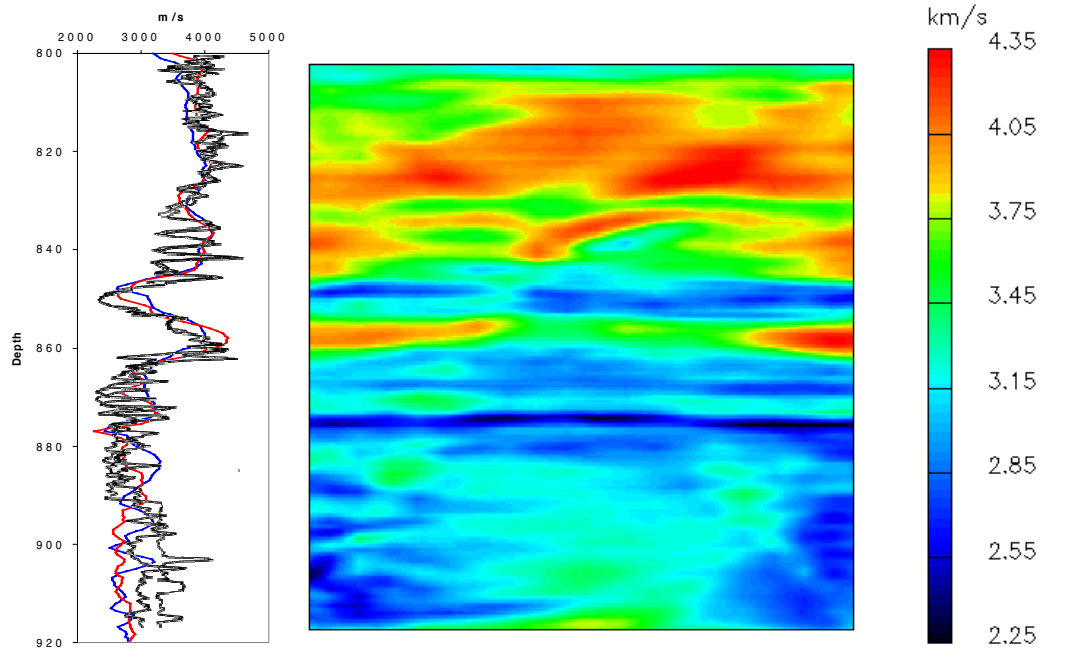

Figure 5: Final isotropic waveform inversion result. The result at the well locations (red = receiver well) is shown on the left together with the original sonic velocities (black).